Transfer Functions of Amplitude and Phase Fluctuations and Additive Noise in Varactor Doublers

ELIO BAVA, GIAN PAOLO BAVA, ALDO GODONE, AND GIOVANNI RIETTO

Abstract—**In order to evaluate the spectral purity degradation produced by varactor doublers, the transfer properties of amplitude and phase fluctuations have been determined with reference to a theoretical analysis developed in a previous work. Quasi-stationary conditions have been assumed and the input and output tuning circuits have been approximated with a linear relation between frequency and reactance. The effect of the bias circuit has been taken into account both for fixed-bias and self-bias conditions. Then the additive-noise contribution of the doubler circuit elements have been obtained. Numerical examples and curves are given for all the evaluated quantities.**

I. Introduction

In a previous paper [1] the nonlinear static behavior (AM–PM and AM–AM conversion) in varactor doublers and triplers has been analyzed, and a few experimental results have been reported in [2].

In order to evaluate the spectral purity degradation of signals at the multiplier output, it is necessary to know the transfer properties of amplitude and phase fluctuations versus the Fourier angular frequency Ω. This determination is developed here for a doubler assuming quasi-stationary conditions (slow fluctuations), and approximating input and output tuning circuits with a linear relation between frequency and reactance. Then the additive noise due to losses in the diode and in the circuit and to shot effect is calculated. This last source of noise appears to be the most important in self-bias operation. Therefore, transistor multipliers, though offering gain advantages, are rather inferior as regards noise performance, owing to the much higher currents at the working point.

II. Dynamic Behavior of a Varactor Doubler

The transfer properties of fluctuations and the noise characteristics have been studied with reference to the circuit of Fig. 1, where

$$V_g = v_g(t)\cos\left[\omega_1 t + \varphi_g(t)\right] \tag{1}$$

and,assuming a "shunt-diode" mode operation, the charge q in the varactor is given by

$$q = q_0 + Q_1' + Q_2'. \tag{2}$$

Manuscript received July 10, 1978; revised February 16, 1979. This work was supported by the Italian National Research Council.

E. Bava, A. Godone, and G. Rietto are with the Istituto Elettrotecnico Nazionale "Galileo Ferraris", Torino, Italy.

G. P. Bava is with the Istituto di Elettronica e Telecommunicazioni del Politecnico, Torino, Italy.

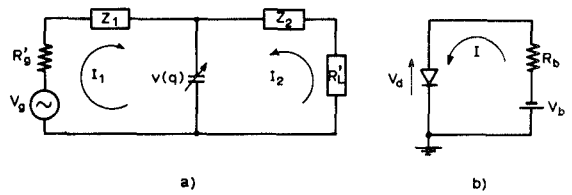

Fig. 1. (a) RF equivalent circuit of a varactor frequency doubler. (b) bias network.

$$Q_i' = q_i(t)\sin\left[\omega_i t + \varphi_i(t)\right] \tag{3}$$

with $i = 1,2$, and $\omega_2 = 2\omega_1$.

If $v_g(t)$ and $\varphi_g(t)$ are fluctuating slowly with respect to the angular frequency ω_1, and when the impedances Z_i can be approximated with the equivalent series resonator near ω_i, $[Z_i = R_i + jX_i = R_i + j(\omega_i L_i - (1/\omega_i C_i))]$, the dynamic behavior of the doubler can be obtained from the first four equations of system (4) given in [1], with subscript "out" $=2$. The quasi-stationarity requirement holds when $\Omega \ll 2\pi B$, where Ω is the Fourier angular frequency of fluctuations ($d/dt = j\Omega$ in eq. (4), [1]) and $B = R_i/(2\pi L_i)$ is the bandwidth of the mesh at ω_i.

Moreover, for an abrupt-junction varactor, the functions F_c^1, F_c^2, F_s^1, and F_s^2 are given by the first four equations of system (6) in [1], by letting $q_3 = 0$.

In metrological applications (high-spectral purity) and in some communication systems, $v_g(t)$ fluctuations are very small compared with the mean value ($|\Delta v_g| \ll v_{g0}$), whereas $|\Delta\varphi_g| \ll 1$ rad, therefore, eqs. (4) and (6) of [1] will be linearized. Another equation must be added to take into account the effect of the bias circuit. Two different expressions hold depending on the fixed-bias or self-bias condition of the diode. In the former case differentiating eq. (10) of [1] with $q_{30} = 0$ gives the wanted equation immediately, whereas for self-bias a more complex procedure is required, that is, differentiating eq. (9) of [1] and at the same time taking into account the diode rectifying characteristic $I(V)$.

Introducing $R_g = R_g' + R_1$, $R_L = R_L' + R_2$, $\varphi_0 = \varphi_{20} - 2\varphi_{10}$, where the quantities with subscript "0" define the static working point, indicating with Δ the deviations from the working point, with Q_1 and Q_2 the quality factors of the two meshes ($Q_1 = \omega_1 L_1/R_g$, $Q_2 = \omega_2 L_2/R_L$), and setting $m = 1/4C_0^2 V_0$ (C_0 is the zero-bias capacitance and V_0 is

0018-9480/79/0800-0753$00.75 ©1979 IEEE

the barrier contact potential), the following linearized equations hold:

$$\frac{\Delta q_1}{q_0}\left(1+j4Q_1\frac{\Omega}{\omega_2}-\frac{2mq_{20}}{\omega_2 R_g}\cos\varphi_0\right)-\frac{\Delta q_2}{q_0}\frac{2mq_{10}\cos\varphi_0}{\omega_2 R_g}$$
$$+\Delta\varphi_1\left[\frac{2v_{g0}}{\omega_2 R_g q_0}\sin(\varphi_{10}-\varphi_{g0})\right.$$
$$\left.-\frac{4mq_{10}q_{20}\sin\varphi_0}{\omega_2 R_g q_0}+j\frac{\Omega}{\omega_2}\frac{2q_{10}}{q_0}\right]+\Delta\varphi_2\frac{2mq_{10}q_{20}\sin\varphi_0}{\omega_2 R_g q_0}$$
$$=\frac{2\Delta v_g}{\omega_2 R_g q_0}\cos(\varphi_{10}-\varphi_{g0})+\frac{2v_{g0}}{\omega_2 R_g q_0}\Delta\varphi_g\sin(\varphi_{10}-\varphi_{g0})$$

$$\frac{\Delta q_1}{q_0}\left(\frac{2mq_{20}\sin\varphi_0-4mq_0}{\omega_2 R_g}-\frac{X_1}{R_g}+j2\frac{\Omega}{\omega_2}\right)+\frac{\Delta q_2}{q_0}\frac{2mq_{10}}{\omega_2 R_g}$$
$$\cdot\sin\varphi_0+\Delta\varphi_1\left[-\frac{2v_{g0}}{\omega_2 R_g q_0}\cos(\varphi_{10}-\varphi_{g0})\right.$$
$$\left.-\frac{4mq_{10}q_{20}\cos\varphi_0}{\omega_2 R_g q_0}-j4Q_1\frac{q_{10}}{q_0}\frac{\Omega}{\omega_2}\right]$$
$$+\Delta\varphi_2\frac{2mq_{10}q_{20}\cos\varphi_0}{\omega_2 R_g q_0}-\frac{\Delta q_0}{q_0}\frac{4mq_{10}}{\omega_2 R_g}$$
$$=\frac{2\Delta v_g}{\omega_2 R_g q_0}\sin(\varphi_{10}-\varphi_{g0})-\frac{2v_{g0}}{\omega_2 R_g q_0}\Delta\varphi_g\cos(\varphi_{10}-\varphi_{g0})$$

$$\frac{\Delta q_1}{q_0}\frac{mq_{10}}{\omega_2 R_L}\cos\varphi_0+\frac{\Delta q_2}{q_0}\left(1+j2Q_2\frac{\Omega}{\omega_2}\right)+\Delta\varphi_1\frac{mq_{10}^2}{\omega_2 R_L q_0}$$
$$\cdot\sin\varphi_0+\Delta\varphi_2\left(-\frac{mq_{10}^2}{2\omega_2 R_L q_0}\sin\varphi_0+j\frac{q_{20}}{q_0}\frac{\Omega}{\omega_2}\right)=0$$

$$\frac{\Delta q_1}{q_0}\frac{mq_{10}}{\omega_2 R_L}\sin\varphi_0+\frac{\Delta q_2}{q_0}\left(-\frac{X_2}{R_L}-\frac{2mq_0}{\omega_2 R_L}+j\frac{\Omega}{\omega_2}\right)$$
$$+\Delta\varphi_1\frac{-mq_{10}^2}{\omega_2 R_L q_0}\cos\varphi_0+\Delta\varphi_2\left(\frac{mq_{10}^2}{2\omega_2 R_L q_0}\cos\varphi_0\right.$$
$$\left.-j2Q_2\frac{q_{20}}{q_0}\frac{\Omega}{\omega_2}\right)-\frac{\Delta q_0}{q_0}\frac{2mq_{20}}{\omega_2 R_L}=0$$

$$2q_0\Delta q_0+q_{10}\Delta q_1+q_{20}\Delta q_2$$
$$+\frac{R_b I_s}{\pi V_T}\int_0^{2\pi}q(t)e^{v(q)/\eta V_T}\Delta q\,d(\omega_1 t)=0 \qquad (4)$$

for self-bias operation. R_b is the bias resistance, I_s is the saturation current, and V_T is the diode volt equivalent of temperature, $q(t)=q_0+q_1\sin(\omega_1 t+\varphi_1)+q_2\sin(2\omega_1 t+\varphi_2)$, and Δq is obtained by differentiating $q(t)$ with respect to q_0, q_1, q_2, φ_1, and φ_2.

If fixed-bias voltage is used, the last equation of system (4) holds with $R_b=0$. System (4) may be used to analyze the behavior of the multiplier as regards possible instabilities, to determine the transfer of fluctuations and to evaluate the additive noise.

Problems of this kind have been studied by many authors for various multiplication orders, but with simpler circuit models [3]–[7].

III. Numerical Calculations of Fluctuation Transfer Functions

For a 500 MHz–1 GHz doubler, whose static behavior, analyzed as reported in [1], is summarized in Table I (maximum efficiency at $P_{av}=1$ W), system (4) has been solved and all input–output transfer functions have been evaluated in self-bias condition for $P_{av}=0.5$, 1, and 2 W. The case $P_{av}=0.5$ W is given here only as an example, since at this level the efficiency, which has been maximized at 1 W by a proper choice of circuit components, drops to a very low value (see fig. 4 of [1]).

In Fig. 2 the modulus and phase of the PM–PM transfer function versus the normalized Fourier angular frequency Ω/ω_2 are given. In this figure and in the following ones a vertical line shows the Ω/ω_2 value corresponding to $\Omega=2\pi B$ (see Section II).

For low Fourier frequencies the transfer function obviously approaches the modulus 2 and the phase 0°. For increasing Ω the shape of the curve is influenced by the Q's of the resonant circuits.

The curves of Fig. 3 refer to the AM–AM transfer function for relative amplitude fluctuations.

For increasing input power a saturation effect is noticeable; moreover, at the maximum efficiency level (1 W) the AM–AM modulus is slightly greater than 1. The limiting value for $\Omega\to 0$ is given by

$$\lim_{\Omega\to 0}\left|\frac{v_2/v_{20}}{v_g/v_{g0}}\right|=\frac{2R_g'}{2R_g'-R_1}=\begin{cases}1, & \text{if } R_1=R_2=0\\ 2, & \text{if } R_1,R_2\to\infty\end{cases}$$

according to the first and third equation of (4) and to (A2) of [1].

In Fig. 4 the PM–AM conversion coefficient is shown; for Ω approaching 0 the linear variation of the modulus is evident.

Fig. 5 reports the AM–PM conversion coefficient (continuous lines). The most unfavorable situation corresponds to the power level chosen for efficiency maximization and in the practical case examined the conversion is rather important. The AM–PM conversion coefficient referred to the input (i.e., divided by the multiplication factor $n=2$), indicated as k' in [2], is 18°/dB. In order that the AM–PM effects be negligible with respect to the natural degradation expressed by PM–PM, the following condition, proved in [2], is necessary:

$$k'(\Omega)\ll\frac{9\ln 10}{\pi}\sqrt{\frac{S_\varphi(\Omega)}{S_\alpha(\Omega)}} \qquad (5)$$

where S_α and S_φ are the spectral densities of the amplitude and phase fluctuations of the input signal.

The best 5-MHz quartz oscillators available at present, have

$$S_\varphi\simeq 10^{-18}\frac{\text{rad}^2}{\text{Hz}}\quad\text{at}\quad\frac{\Omega}{2\pi}=1\text{ kHz}$$

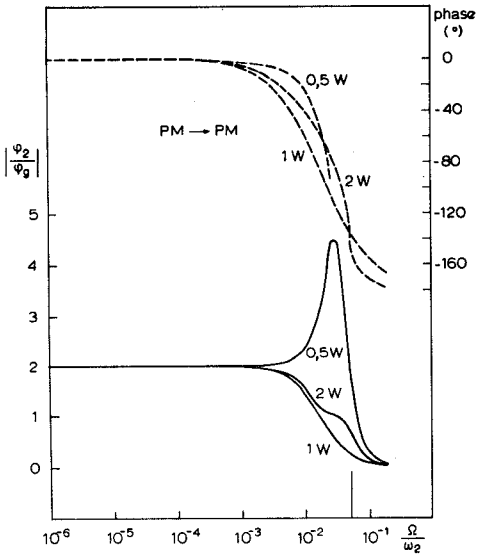

Fig. 2. PM–PM transfer functions (φ_2/φ_g). Maximum efficiency at 1 W, input frequency 500 MHz: continuous lines = modulus; dashed lines = phase.

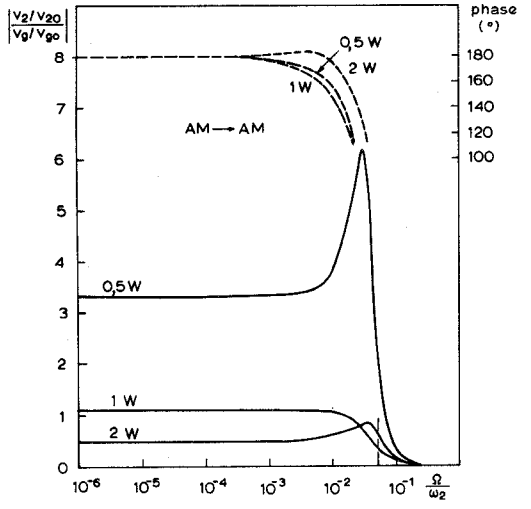

Fig. 3. AM–AM transfer functions ($(v_2/v_{20})/(v_g/v_{g0})$). Maximum efficiency at 1 W, input frequency 500 MHz: continuous lines = modulus; dashed lines = phase.

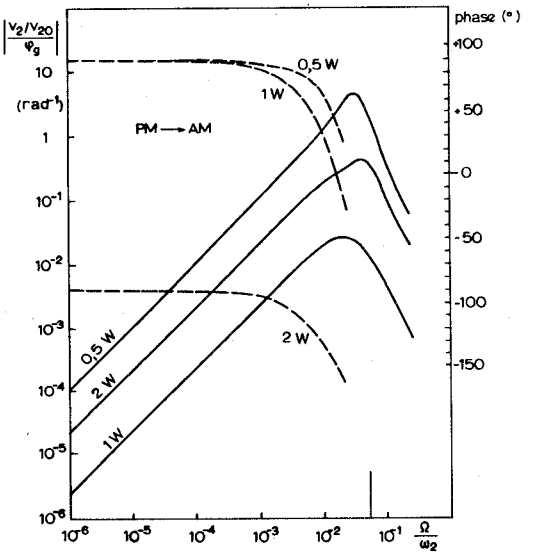

Fig. 4. PM–AM transfer functions ($(v_2/v_{20})/\varphi_g$). Maximum efficiency at 1 W, input frequency 500 MHz: continuous lines = modulus; dashed lines = phase.

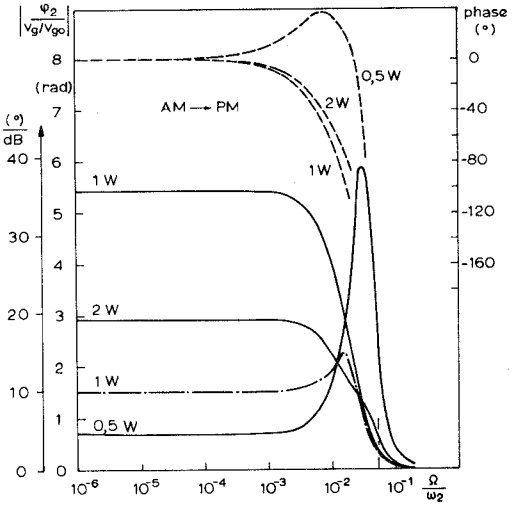

Fig. 5. AM–PM transfer functions ($\varphi_2/(v_g/v_{g0})$). Maximum efficiency at 1 W, input frequency 500 MHz: continuous lines = modulus; dashed lines = phase; dot-and-dash line = modulus for fixed bias.

and

$$S_{\alpha,\min} \simeq 4 \times 10^{-19}\ \mathrm{Hz}^{-1}$$

(due to thermal noise alone). Transferring these data to $f_1 = 100$ MHz, it is found from (5) that $k'(\Omega) \ll 209.1°/\ \mathrm{dB}$.

This evaluation is optimistic since it does not take into account the increase in S_α, due to the additive noise and to the AM–AM transfer ratio in the preceding stages.

Since there is at present a trend to build high-spectral purity quartz oscillators operating at 100 MHz with characteristics similar to those indicated above at 5 MHz, condition (5) should become

$$k'(\Omega) \ll \frac{209.1}{20}\ °/\mathrm{dB} = 10.45°/\mathrm{dB}$$

which is very strict as regards the AM–PM performance required from the doubler. The improvement achievable

TABLE I
CIRCUIT VALUES AND STATIC PARAMETERS OF THE ANALYZED DOUBLER; THE PHASES ARE EVALUATED FOR $\varphi_{g0} = 0$

P_{av} [W]	$q_0 \times 10^{10}$ [C]	$q_{10} \times 10^{10}$ [C]	$q_{20} \times 10^{11}$ [C]	φ_{10} (°)	φ_{20} (°)
0.5	- 0.65948	+ 0.44867	0.33369	-73 .257	-12 .3074
1	- 1.74056	1.34734	4.31578	0	180
2	- 2.13027	1.56808	5.48148	27 .4454	255 .225

$V_T = 0.04$ [V] $\quad f_1 = 500$ MHz
$R_b I_s = 0.1$ [V] $\quad R_1 = 2\ \Omega$
$m = 6.67 \times 10^{20} \quad R_2 = 2\ \Omega$
$V_0 = 0.6$ [V] $\quad P_{av,\eta max} = 1$ W

$R_g' = 11.163\ \Omega \quad X_1 = 73.9087\ \Omega \quad Q_1 = 20$
$R_L' = 20.326\ \Omega \quad X_2 = \frac{X_1}{2} \quad Q_2 = 20$

with output circuit detuning (fig. 6, [1]) is not enough to satisfy the above inequality.

A more interesting way of reducing the AM–PM conversion is to bias the diode with a fixed reverse voltage. In this case the PM–PM, PM–AM, and AM–AM transfer functions are not affected appreciably, whereas the AM–PM conversion is greatly reduced, as shown by the dash-and-dot curve of Fig. 5; in this case the AM–PM conversion coefficient referred to the input is reduced to about 5°/dB.

IV. Additive Noise

The main sources of additive noise in the multiplier of Fig. 1, assuming that the diode is never operating in the breakdown region, are the following:

thermal noise due to the series resistance of the varactor and the tuning circuits and to the bias resistance;
flicker noise, for very low Ω's;
shot noise due to the self-bias current;
possible fluctuations of the fixed-bias voltage.

The output noise spectra (bandwidth = 1 Hz) are calculated by replacing the known terms of system (4) with the quantities A_i (see Table II) representing the equivalent noise sources (A_i refers to the ith equation of system (4)). Since the different noise sources are uncorrelated, their noise power contributions at the output must be evaluated separately, and then summed.

The output amplitude and phase fluctuations due to R_1 and R_2 thermal noise for the maximum efficiency case $P_{av} = 1$ W (Table I) are reported in Fig. 6, both for self- and fixed-bias conditions.

It appears that the power spectral densities produced by R_1 have a slightly narrower band than those produced by R_2 and exhibit a faster decay outside the band. This is due to the more effective filtering of the noise originated in the input mesh. It may be remarked also that in self-bias conditions, the phase noise due to R_1 and R_2 is decidedly more important than the amplitude noise. This latter does not change significantly when fixed bias is used, whereas in this case, there is an improvement in the phase noise spectrum which, moreover, decreases with V_b as it appears from the solution of system (4).

The improvement in phase noise produced by fixed-bias results from the lower AM–PM conversion coefficient, as indicated in the preceding section.

The noise spectra due to the bias network are shown in Fig. 7. In the case of self bias a value of 100 kΩ has been chosen for R_b. The effect of external bias voltage fluctuations is negligible. In order to make its spectrum visible in Fig. 7, for the spectral density of fluctuations the greatly exaggerated value of 1 mV/$\sqrt{\text{Hz}}$ has been assumed.

The effects of R_b thermal noise on amplitude fluctuations are negligible; the phase noise is of the same order as that generated by R_1 and R_2. Since the bias network operates near zero frequency, the contribution of flicker noise may be important. The diagrams of Fig. 7 can be

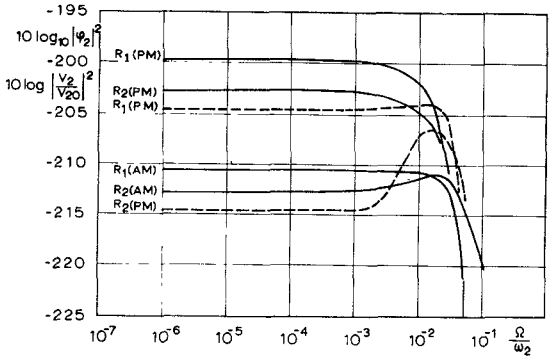

Fig. 6. Output spectra of amplitude and phase fluctuations due to thermal noise of spreading resistances R_1 and R_2; the same vertical scale is used for both spectra. For phase noise continuous lines, refer to self-bias operation, and dashed lines to fixed bias [$V_b = 30$ V]. For amplitude noise there is no difference between the two conditions.

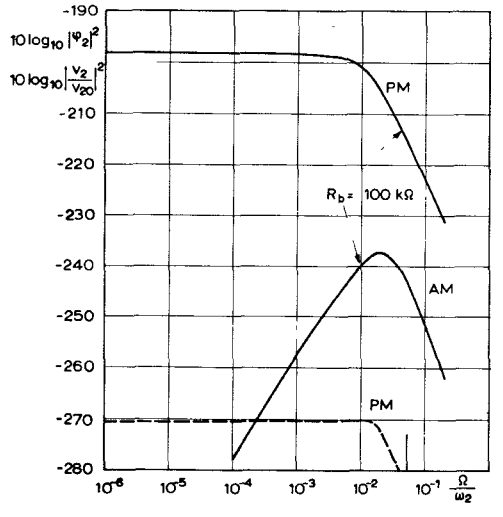

Fig. 7. Output fluctuations due to the bias circuit; the same vertical scale is used for amplitude and phase spectra. The continuous lines are the contribution of thermal noise in the bias resistance R_b. The dashed line is the contribution due to fluctuations of an external voltage assuming a white noise of 1 mV/$\sqrt{\text{Hz}}$.

TABLE II

Known Terms A_i of System (4) Taking into Account the Sources of Additive Noise; k = Boltzmann Constant, T = Absolute Temperature

thermal noise due to R_1	$\left.\begin{matrix}A_1\\A_2\end{matrix}\right\} = \frac{\sqrt{2}}{\omega_1 R_g \lvert q_0\rvert}$	$\sqrt{4kTR_1}$
thermal noise due to R_2	$\left.\begin{matrix}A_3\\A_4\end{matrix}\right\} = \frac{\sqrt{2}}{\omega_2 R_L \lvert q_0\rvert}$	$\sqrt{4kTR_2}$
thermal noise due to R_b	$A_5 = \frac{\sqrt{4kTR_b}}{2m\lvert q_0\rvert}$	
bias voltage fluctuations (fixed bias)	$A_5 = \frac{\Delta V_b}{2m\lvert q_0\rvert}$	

used to evaluate the effects of R_b flicker noise, by denormalizing with respect to thermal noise and multiplying by the spectral density of the flicker noise.

The shot noise, due to the self-bias current, gives contributions around the angular frequencies $\omega \simeq 0$, $\omega \simeq \omega_1$, $\omega \simeq \omega_2$. Their effect on the output fluctuations ($\omega \simeq \omega_2$) can be obtained from the curves of Fig. 7 ($\omega \simeq 0$) and Fig. 6, by multiplying their respective results by the following factors:

$$\frac{R_b}{2V_T}(I+2I_s) \qquad \text{(curves showing } R_b \text{ contribution)}$$

$$\frac{R_g^2}{2R_1V_T}(I+2I_s) \qquad \text{(curves showing } R_1 \text{ contribution)}$$

$$\frac{R_L^2}{2R_2V_T}(I+2I_s) \qquad \text{(curves showing } R_2 \text{ contribution)}$$

where I is the diode mean current.

It is evident that the first quantity is quite large (in our example it is approximately 320) and, therefore, one may conclude that, at least for phase fluctuations under self-bias conditions, the shot-noise contribution is by far the most important one.

The resistive characteristic of the diode has been used only for self-bias calculations. The related resistive mixing effects have not been taken into account in calculating both the signal fluctuations and the additive noise. However, it is to be remarked that the efficiency of resistive mixing is sensibly lower than that of the varactor effect.

V. Conclusion

In the first part of this work the transfer functions for amplitude and phase fluctuations in an abrupt-junction varactor doubler have been analyzed and calculated.

The evaluation of AM–PM conversion appears to be of special importance; in particular, this quantity may be significant in a self-biased multiplier, and is greatly reduced when external bias with fixed voltage is used.

Then the additive noise contributions produced by the circuit elements have been calculated. In a self-biased multiplier, without breakdown, the most important contribution to the additive noise is given by the shot noise in the diode detected current. Here again this effect can be made negligible by using fixed bias.

References

[1] E. Bava, G. P. Bava, A. Godone, and G. Rietto, "Analysis of varactor frequency multipliers: non linear behavior and hysteresis phenomena," *IEEE Trans. Microwave Theory Tech.*, vol. MTT-27, Feb. 1979.

[2] E. Bava, G. P. Bava, A. De Marchi, and A. Godone, "Measurement of static AM–PM conversion in frequency multipliers," *IEEE Trans. Instrum. Meas.*, vol. IM-26, pp. 33–38, Mar. 1977.

[3] V. K. Prabhu, "Noise performance of abrupt junction varactor frequency multipliers," *Proc. IEEE*, vol. 54, pp. 285–287, Feb. 1966.

[4] C. Dragone, "Phase and amplitude modulation in high efficiency varactor frequency multipliers—General scattering properties," *Bell Syst. Tech. J.*, vol. 46, pp. 775–796, Apr. 1967.

[5] ——, "Phase and amplitude modulation in high efficiency frequency multipliers of order $N=2^n$, stability and noise," *Bell Syst. Tech. J.*, vol. 46, pp. 797–834, Apr. 1967.

[6] C. Dragone and V. K. Prabhu, "Scattering relations in lossless varactor frequency multipliers," *Bell Syst. Tech. J.*, vol 46, pp. 1699–1781, Oct. 1967.

[7] G. B. Stracca, "Osservazioni sul progetto dei moltiplicatori di frequenza a varactor," *Alta Frequenza*, vol. 40, pp. 10–27, Jan. 1971.